ANNUAL TECHNICAL PROGRESS REPORT FOR

Title: Nanostructured High Performance Ultraviolet and Blue Light Emitting Diodes for Solid State Lighting*
Type of report: Annual
Reporting Period: October 1, 2003 to September 30, 2004
Principal Authors: Professor Arto V. Nurmikko (Brown University) and Professor Jung Han (Yale University)
Date Report was Issued: October 2004
DOE Award Number: DE-FC26-03NT41941

ABSTRACT

We report on research results in this project which synergize advanced material science approaches with fundamental optical physics concepts pertaining to light-matter interaction, with the goal of solving seminal problems for the development of very high performance light emitting diodes (LEDs) in the blue and near ultraviolet for Solid State Lighting applications. Accomplishments in the first 12 month contract period include (i) new means of synthesizing zero- and one-dimensional GaN nanostructures, (ii) establishment of the building blocks for making GaN-based microcavity devices, and (iii) demonstration of top-down approach to nano-scale photonic devices for enhanced spontaneous emission and light extraction. These include a demonstration of eight-fold enhancement of the external emission efficiency in new InGaN QW photonic crystal structures. The body of results is presented in this report shows how a solid foundation has been laid, with several noticeable accomplishments, for innovative research, consistent with the stated milestones.

TABLE OF CONTENTS

LIST OF GRAPHICAL MATERIALS

All graphical materials are imbedded within the main body of this report

EXECUTIVE SUMMARY

The stated aim of this research is to synergize advanced material science approaches with fundamental optical physics concepts pertaining to light-matter interaction, with the goal of solving seminal problems for the development of very high performance light emitting diodes (LEDs) in the blue and near ultraviolet for Solid State Lighting applications, covering the spectral regime of approximately 370-480 nm. Our mission is to implement novel, highly adaptable device concepts that enable their flexible utilization and matching to the broad spectrum of approaches and requirements that pertain to contemporary solid state lighting approaches. The light emitters will be based on nanostructured gallium nitride and related semiconductor heterostructures, which are enclosed by mesoscopic optical confinement and directional housings. The proposed research aims to reach the goal of a highly wall-plug efficient, high optical power device by concentrating on two specific, closely coupled performance dictating elements within the LED.

The research program has been organized in the following way: First, we are synthesizing nanostructured active media to enhance the internal radiative efficiency, by utilizing special concepts in epitaxial growth for synthesizing quantum dots and quantum wires. During the first 12 month contract period we have made substantially advances in the synthesis of zero- and one-dimensional GaN nanostructures by crystal growth technique that exploits a vapor-liquid-solid nucleation pathway. Second, the research has also focused focus on the design and fabrication of advanced photonic confinement structures, which encase the nanostructured active medium for enhancing the spontaneous emission by strengthening light-matter interaction at a fundamental level and for efficiently extracting and distributing the photons for delivery into specific geometrical radiation patterns by design. During the first 12 month period we have established the fabrication means for key building blocks for making GaN-based microcavity devices. In addition, novel light emitting structures, with active element feature size on the subwavelength scale have been fabricated and tested. These include a demonstration of eight-fold enhancement of the external emission efficiency in new InGaN QW photonic crystal structures.

I. INTRODUCTION

A revolution in lighting regarding energy saving, component lifetime, and fixture versatility is anticipated if the traditional tube-based (incandescent and fluorescent) lamps can be replace by solid state LEDs. For this vision to become reality, a substantial gap in terms of light output between a standard incandescent bulb (1000~2000 lumens) and a single III-N LED chip (1~5 lumens) needs to be bridged. Engineering issues such as metal contacts, current spreading, and light extraction have to be addressed in scaling up the device area for increased optical output from a single chip. Of paramount importance is the identification and realization of an active medium capable of more efficient conversion of electron-hole pairs into photons, especially under higher-level current injection ($J=10^3 \sim 10^4$ A/cm^2). Carrier localization due to In-related compositional fluctuations in InGaN is attributed to the constraint of in-plane carrier diffusion, thus preserving and preventing the injected carriers from recombining at nonradiative dislocation sites. Such a benefit of localization diminishes at high-level injection as more carriers acquire a nature of extended electronic states and are consumed by nonradiative processes. A recent observation of a substantial decay in quantum efficiency at a modest injection level from state-of-the-art high power AlGaInN LEDs[1] served as a reminder of the necessity of innovative and creative material research for an efficient light-emitting medium.

In this report we summarize the progress made during the first year of the DOE Contract entitled "Nanostructured High Performance Ultraviolet and Blue Light Emitting Diodes for Solid State Lighting". Details of the experimental facilities and methodology are described in experimental section (II). The body of results is presented in Section III which clearly indicated that a solid foundation has been laid, in additional to several noticeable accomplishments, for reaching the stated milestones in the coming years. Specifically we have made substantially advances in the synthesis of zero- and one-dimensional GaN nanostructures, established the building blocks for making GaN-based microcavity devices, and demonstrated a top-down approach to nano-scale photonic devices for enhanced spontaneous emission and light extraction.

II. EXPERIMENAL

MOCVD growth was carried out in a horizontal reactor (Aixtron 200/4 HT-S) using trimethylgallium (TMGa), trimethylaluminum (TMAl), and ammonia (NH_3) as sources with hydrogen as the carrier gas. 0.9 μm thick $Al_{0.26}Ga_{0.74}N$ and $Al_{0.40}Ga_{0.60}N$ templates, with a mismatch to GaN that is much below the threshold for SK nucleation, were grown on sapphire using a 0.3 μm AlN buffer.[2] After the growth of AlGaN at 1080°C, growth was interrupted under a flow of ammonia and the temperature was reduced to 600 °C for the deposition of gallium to take place. Atomic force microscopy (AFM) was conducted using a Digital Instrument Nanoprobe III model with tapping mode. AFM of the AlGaN reveals a step flow growth pattern with a typical pit density between 10^9 and 10^{10} cm^{-2}. PL signal was collected using a 30 ns pulsed frequency-quadrupled Nd:YAG laser emitting at 266 nm. Scanning electron microscopy (SEM) was performed using a LEO 1530 Field Emission SEM. High-resolution transmission electron microscopy (TEM) and electron diffraction (ED) were performed using a FEI Tecnai 20 Field Emission

TEM. Scanning energy dispersive x-ray spectrometry (EDS) was carried out in a Philips CM-12 TEM with a nominal beam diameter of 50 nm.

III. RESULTS AND DISCUSSION

III.A. GaN quantum dots

The spontaneous formation of InGaN nanostructures during heteroepitaxy on GaN represents a fortuitous provision from nature which is responsible for the carrier localization and achieving high brightness blue light emitting diode (LED) operation with an otherwise dislocated active region.[3] The observed nanoscale fluctuation in InGaN alloy composition derives its physical origin from heteronucleation under an excessive compressive strain. A transition from the initial two-dimensional (2D) layer-by-layer growth to three-dimensional (3D) islands, commonly referred to as the Stranski-Krastanov (SK) nucleation mode,[4] constitutes another mechanism of strain-driven nucleation of nanoscale structures and has been a subject of intense study for both technological and scientific reasons. Self-assembled InAs quantum dots (QDs) provide access to the 1.3-1.55 μm wavelength on GaAs substrates with a reduced threshold current density.[5] Delta-function like density-of-states distribution associated with zero-dimensional QDs enables a mesoscopic embodiment of artificial atoms with unique application such as single electron devices and single photon emitters.[6] In addition to the obvious advantage of enhancing radiative recombination through carrier localization, controlled synthesis of GaN and AlGaN QDs will create a crucial linkage of ultraviolet (UV) nanophotonics with biological applications.

The use of SK nucleation mode necessitates the employment of a template with a much smaller lattice constant; strained nucleation of GaN QDs on AlN has been demonstrated by both molecular beam epitaxy (MBE)[7] and metalorganic chemical vapor deposition (MOCVD).[8] However, highly resistive AlN makes it difficult to achieve the electrical injection of carriers into (Al)GaN QDs. Using silicon as an anti-surfactant, Hirayama et al.[9] has demonstrated the formation of GaN and InGaN on nearly lattice-matched templates. It is speculated that the Si-N bonding and sub-monolayer coverage alters (reduces) the surface energy, thus facilitating the 3D islanding. Similar to previous examples of (anti)surfactants,[10] the incorporation of a high dosage of tetravalent silicon in the atomic vicinity of QDs presents a source for non-radiative recombination.

Near and above its melting point, metallic thin film transforms into nanoscale liquid droplets, a phenomenon that does not require the presence of strain mismatch or surfactant. The formation of metal droplets due to surface tension presents an alternative route to semiconductor nanostructures by converting the droplets into crystalline QDs. Koguchi et al.[11] has demonstrated the formation of nanometer Ga droplets on GaAs substrates and the conversion into GaAs QDs through an exposure to arsenic vapor. Kawasaki et al.[12] and Hu et al.[13] have reported the preparation of GaN QDs on, respectively, AlGaN and SiC by droplet conversion using gas source MBE. Only low temperature luminescence was observed in these samples; a deviation of microscopic stoichiometry was identified as a factor compromising the recombination efficiency. In this work we demonstrate that gallium droplet heteroepitaxy (DHE) is a valid path toward the flexible synthesis of GaN QDs with high optical efficacy. The formation of Ga

droplets, including the nucleation dynamics and kinetics, is examined at the atomic scale. The conversion of gallium droplets upon exposure to ammonia proceeds with two competing mechanisms, a liquid-phase-epitaxy-like crystallization of quantum dots and the diffusion-based two-dimensional growth of GaN layers, both can be regulated by surface kinetics. Photoluminescence (PL) at 345 nm at room temperature suggests that the converted QDs are optically active and can be a candidate for ultraviolet emitters.

A detailed understanding of the formation and evolution of gallium nanodroplets forms the foundation of the current work. Ga deposition was achieved by flowing TMGa in the absence of ammonia; the ammonia flow was interrupted two minutes prior to TMGa flow to avoid unintentional growth of GaN. The flow of TMGa (4 to 40 μmole/min) and the duration of deposition (7.5 to 120 seconds) were used to control the

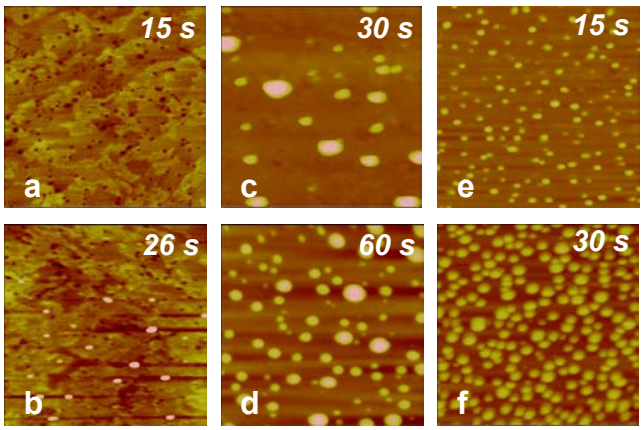

Figure 1. 1x1 μm^2 AFM images illustrating the evolution of Ga deposits on AlGaN, TMGa flow is 4.4 μmol/min for (a,b,c,d) and 8.8 μmol/min for (e,f); deposition time is shown on the images; vertical gray scale is 5 nm for (a,b) and 50 nm for (c,d,e,f).

nucleation dynamics. At the lowest TMGa flow of 4.4 μmol/min, initial deposition of Ga proceeds through an occurrence of Ga bilayers[14,7] near the surface steps of AlGaN with a height of around 6 Å, covering approximately 40 % of the surface (bright regions in Fig. 1a). Beyond an equivalent (integrated) thickness of approximately 2.5 Å, an onset of the formation of Ga nanodroplets was observed (Fig. 1b), juxtaposing with the background Ga bilayers even though the coverage of bilayers is estimated to be less than 50 %. Further increase in deposition time to 30 and 60 s leads to the increase in droplet density (Fig. 1c,d), followed by the increase in island size once the density saturates at about $1x10^{10}$ cm^{-2}, as the time of deposition is increased to 120 s (not shown). The morphology of Ga nanodroplets resulting from 30 and 60 s of TMGa exposure at 4.4 μmol/min is characterized by a distribution of island diameters between 10 (close to the lower limit of resolution) and 80 nm, and the average aspect ratio of ¼ (the ratio of the island height to its diameter).

The dynamics of the formation of Ga nanodroplets involves kinetic processes such as heterogeneous nucleation, surface diffusion, and concurrent ripening through grain growth.[15,16] Theoretical modeling[17] has predicted the coexistence of monodispersed large droplets, regulated by the ripening process, with polydispersed small droplets as a result of continuous nucleation. Figures 1e and 1f show the morphology of Ga nanodroplets deposited with twice the flow rate and half the flow duration, as compared to Fig. 1c and 1d. As the flow of TMGa is increased, the nucleation barrier for droplet formation is reduced as a result of increased supersaturation, thereby leading to higher island densities, while the nominal thickness is preserved. Considerable narrowing of droplet size distribution is also observed with the reduction in the deposition time (Fig.

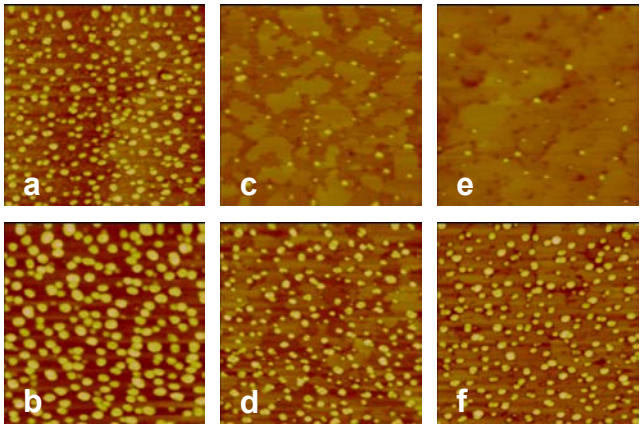

Figure 2. 1x1 μm^2 AFM images of converted GaN layers, the starting Ga morphology is shown in Fig. 1e for the top row, and Fig. 1f for the bottom row; (a,b) GaN QDs after NH_3 exposure at 600 °C; (c,d) GaN QDs further subjected to a temperature ramp to 750 °C; (e,f) AlGaN-capped GaN QDs; vertical gray scale is 20 nm in all cases.

1e,f). A prudent selection of growth parameters such as temperature, supersaturation, and extent of ripening is expected to produce Ga droplets with controlled density and homogeneity.

Conversion of Ga nanodroplets into GaN quantum dots was preformed by exposing the Ga droplets to ammonia flow immediately after the TMGa flow, followed by a rapid cooling of the samples under NH_3 flow. The conversion process represents an interplay between several competing mechanisms. The first is the reaction of nitrogen with gallium nanodroplets, resulting in the formation of a supersaturated solution and consequently the crystallization of GaN at the droplet/AlGaN interface. On the other hand, the transition from nanodroplets to crystal can proceed differently when Ga adatoms have a high surface diffusion rate; the diminishing role of the surface tension as Ga droplets solidify in the absence of a high compressive strain makes it possible for the Ga atoms to diffuse out from the droplets and participate in a layer-by-layer growth.[18] Based on the notion that the kinetic barriers associated with surface diffusion can be modified by the local surface stoichiometry,[19] the effect of ammonia flow during conversion was investigated in a series of preliminary experiments. It was demonstrated that the initial density of Ga islands ($2.5x10^{10}$ cm^{-2}) is preserved under NH_3 flow of 2000

sccm, while the reduction of flow to 70 sccm leads to one order of magnitude reduction in density, followed by a complete disappearance of 3D features at the expense of the 2D lateral growth of GaN at 4 sccm. The optimization of the density and size of the Ga droplets described earlier resulted in the conditions yielding island densities close to $2x10^{10}$ cm^{-2} and the average size of 22 and 40 nm (Fig. 1e,f). Figure 2 illustrates the morphology of GaN QDs formed as a result of the NH_3 exposure at 2000 sccm. In both cases, the samples were exposed to NH_3 flow at a constant temperature of 600 ºC for 10 seconds and rapidly cooled down under NH_3 flow (Fig. 2a,b).

Having established a process for the preparation of Ga nanodroplets and conversion into GaN QDs (at 600°C), we proceed to investigate the possibility of incorporating the DHE process into regular AlGaN growth procedure which involves a temperature ramp to 750 °C as well the capping of GaN QDs with AlGaN, during which the stability of nanoscale GaN is of particular interest. Fig. 2c and 2d show AFM images of two samples prepared in the same way as those in Fig. 2a and 2b, yet subsequently subjected to a temperature ramp to 750 °C at 5250 sccm of ammonia flow. The QDs in Fig. 2c exhibit a four-fold decrease in density and a reduction in size, with the appearance of flat GaN plateaus of 15 Å height covering approximately 50 % of the surface in the background. In contrast, the density of the QDs is preserved in the case of the larger initial droplet size (Fig. 2d), and the ratio of the integrated volume between aerial GaN plateaus and the QDs is greatly reduced. The instability of small GaN QDs against temperature ramping and annealing is consistent with the curvature-driven capillary phenomena described by the Gibbs-Thomson equation.[15] The presence of patches of GaN "wetting layers" differs from the initial uniform wetting in the SK mode and introduces a new degree of controlling the electronic coupling among the quantum dots. Subsequently, the GaN QDs were capped with a 3 nm thick $Al_{0.24}Ga_{0.76}N$ grown at 750 ºC under the conditions similar to those used in the growth of the active region of the UV

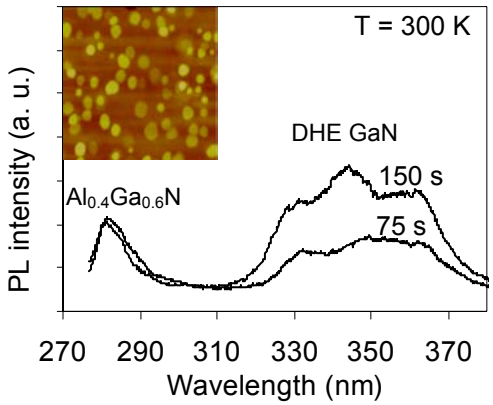

Figure 3. Room temperature photoluminescence spectra of GaN quantum dots that were annealed for 75 and 150 sec before capping with $Al_{0.40}Ga_{0.60}N$ at 960 °C. Inset: 1x1 μm^2 AFM image of AlGaN-capped GaN annealed for 150 sec (20 nm gray scale).

emitters.[2] Further decrease in the density of 3D features is observed in the case of the

small dots (Fig. 2e), while the density of the larger features (Fig. 2f) remains close to $2.5x10^{10}$ cm^{-2}.

Optical properties of GaN obtained by DHE were investigated by PL with a 266 nm excitation source. Room-temperature PL spectra of AlGaN-capped QD samples are shown in Figure 3. To remove the ambiguity in PL peak designation, an $Al_{0.40}Ga_{0.60}N$ template is used which gives rise to a distinct peak at 280 nm. The emission at 345 nm is attributed to the presence of GaN QD structures (AFM is shown in inset), corresponding to the equivalent GaN thickness of approximately 1 nm. We note that the as-converted GaN QDs also yield a distinct PL signal at room temperature (not shown), however, annealing at 960°C before capping with 3 nm of $Al_{0.40}Ga_{0.60}N$ systematically and substantially improves the PL efficiency, suggesting that device-quality low-dimensional structures can be produced using DHE by addressing the issue of microscopic stoichiometry through post-growth annealing.

In conclusion, it has been demonstrated that DHE of GaN on conductive AlGaN templates is a viable path towards UV emitters incorporating zero-dimensional structures in the active region. The evolution of thin Ga films on AlGaN proceeds via the transition from the initial 2D bilayers to the formation of 3D droplets once the critical thickness is reached. Ga island densities and size homogeneity are controlled by manipulating the supersaturation conditions and deposition rate to obtain the densities on the order of 10^{10} cm^{-2} and nanometer-scale droplet size with a narrow distribution suitable for QD conversion. The resulting morphology of the GaN QDs is influenced by the surface kinetics and necessitates the use of the nitrogen-rich conditions to stabilize the GaN islands and prevent 2D growth. Optically active AlGaN-capped QDs exhibiting PL emission at 345 nm at room temperature were obtained by stabilizing the density of the GaN islands throughout the process of DHE and subsequent annealing before AlGaN capping.

[1] J. J. Wierer, D. A. Steigerwald, M. R. Krames, J. J. O'Shea, M. J. Ludowise, G. Christenson, Y. –C. Shen, C. Lowery, P. S. Martin, S. Subramanya, W. Gotz, N. F. Gardner, R. S. Kern, and S. A. Stockman, "High-power AlGaInN flip-chip lght-emitting diodes," Appl. Phys. Lett. **78**, 3379 (2001).

[2] M. Gherasimova, J. Su, G. Cui, J. Han, H. Peng, E. Makarona, Y. He, Y.-K. Song, A. V. Nurmikko, Mat. Res. Soc. Proc. 798, Y1.8 (2004).

[3] S. Chichibu, T. Azuhata, T. Sota, and S. Nakamura, Appl. Phys. Lett. 70, 2822 (1997).

[4] V. A. Shchukin, N. N. Ledentsov, and D. Bimberg, *Epitaxy of Nanostructures* (Springer, Berlin, 2003).

[5] F. Schäfer, J. P. Reithmaier, and A. Forchel, Appl. Phys. Lett. 74, 2915 (1999).

[6] Z. Yuan, B. E. Kardynal, R. M. Stevenson, A. J. Shields, C. J. Lobo, K. Cooper, N. S. Beattie, D. A. Ritchie, and M. Pepper, Science 295, 102 (2002).

[7] N. Gogneau, D. Jalabert, E. Monroy, T. Shibata, M. Tanaka, and B. Daudin, J. Appl. Phys. 94, 2254 (2003).

[8] M. Miyamura, K. Tachibana, and Y. Arakawa, Appl. Phys. Lett. 80, 3937 (2002).

[9] H. Hirayama, S. Tanaka, P. Ramvall, and Y. Aoyagi, Appl. Phys. Lett. 72, 1736 (1998).

[10] E. Tournié, and K. H. Ploog, Thin Solid Films, 231, 43 (1993).

[11] N. Koguchi, K. Ishige, and S. Takahashi, J. Vac. Sci. Technol. B 11, 787 (1993).

[12] K. Kawasaki, D. Yamazaki, A. Kinoshita, H. Hirayama, K. Tsutsui, and Y. Aoyagi, Appl. Phys. Lett. 79, 2243 (2001).
[13] C.-W. Hu, A. Bell, F. A. Ponce, D. J. Smith, and I. S. T. Tsong, Appl. Phys. Lett. 81, 3236 (2002).
[14] J. E. Northrup, J. Neugebauer, R. M. Feenstra, and A. R. Smith, Phys. Rev. B 61, 9932 (2000).
[15] M. Zinke-Allmang, L. C. Feldman, and M. H. Grabow, Surf. Sci. Rep. 16, 377 (1992).
[16] M. Harsdorff, Thin Solid Films 90, 1 (1982).
[17] F. Family and P. Meakin, Phys. Rev. A 40, 3836 (1989).
[18] N. Koguchi, S. Takahashi, and T. Chikyow, J. Cryst. Growth 111, 688 (1991).
[19] M. Gherasimova, G. Cui, Z. Ren, J. Su, X.-L. Wang, J. Han, K. Higashimine, N. Otsuka, J. Appl. Phys. 95, 2921 (2004); T. Zywietz, J. Neugebauer, and M. Scheffler, Appl. Phys. Lett. 73, 487 (1998).

III.B. GaN nanowires

Fueled in part by the discovery of carbon nanotubes,[1] the synthesis of one-dimensional (1D) nanostructures has recently attracted much attention for potential applications in electronic, photonic, and biological areas. Semiconductor nanowires offer unique features such as control of bipolar conductivity and heterojunction bandgap engineering. Si[2] and III-V[3] semiconductor nanowires have been prepared based on catalytic reaction through vapor-liquid-solid (VLS) growth mechanism.[4] Innovative progress has been reported in the bottom-up assembly of these 1D functional components.[5] There is nevertheless a need to enrich the functionality and complexity of the individual building blocks *in-situ* by incorporating the VLS concept into modern heteroepitaxial practices such as molecular beam epitaxy (MBE) and metalorganic chemical vapor deposition (MOCVD).[6,7] To date the synthesis of GaN nanowires are performed primarily by a near-equilibrium, tube furnace technique which does not offer optimum control or flexibility. In this letter we report our observations in preparing III-N nanowires using a conventional MOCVD system. In addition to demonstrating GaN and AlN nanowires from a cold-wall, commercial platform, which has not been reported to our knowledge, we outline the critical issues of nanowire synthesis and present specific solutions. The versatility of using MOCVD for nanowire synthesis is illustrated by the fabrication of three-dimensional (3D) GaN/AlN nano-trees.

The basic principle of VLS mechanism for anisotropic growth of 1D nanostructures was summarized by Wagner.[4] Prerequisites that were identified include: (1) A sizable disparity in reaction kinetics between regular vapor-solid (VS) and the VLS mechanisms, thus mandating a low supersaturation for growth selectivity; (2) the creation and retention of liquid droplets to facilitate adsorption and incorporation of vapor phase species; and (3) the need to have nucleation sites with appropriate crystallographic orientations conducive to the minimization of surface energies. Criterion (1) helps to elucidate the popularity and success in the synthesis of GaN nanowires through hot-wall, flow-tube furnace chamber in which elemental Ga source is placed upstream of catalyst-treated substrates.[8] The proximity of a desorptive source to an adjacent growth surface spontaneously creates an ambient that is close to thermodynamic equilibrium. Favorable conditions for nanowires growth (under low supersaturation) is empirically derived by adjusting the relative positioning between the Ga boat and substrate due to spatial gradients in temperature and Ga flux. On the other hand, modern MOCVD involves a much different and complex process in which organometallic precursors (undersaturated even at room temperature) are transported in vapor phase with minimum dissociation to the vicinity of growth surface. The precursors then undergo rapid pyrolysis decomposition upon entering the heated zone near surface (thermal boundary layer), creating a highly inhomogeneous profile and a mass-transport limited growth process.[9]

Nucleation experiments were carried out initially on catalyst treated surfaces[10] under a constant NH_3 flow of 1000 sccm. Regular vapor-solid nucleation diminishes in agreement with the classical nucleation theory with an increasing temperature and a decreasing flow of TMGa. We note that the existence of liquid-mediated, anisotropic 1D growth depends sensitively on the growth stoichiometry, or V/III ratio, in an MOCVD environment. At the lowest NH_3 flow (~10 sccm), large Ga droplets were observed, accompanied with conical shape GaN "tails" due to VLS crystallization through droplets

with ever-increasing sizes. At an intermediate flow of NH_3, GaN nano-rods with a length up to 0.5 μm and a diameter of 100 nm were observed. The sharpening of the cross-section toward the tip implies a gradual solidification and shrinkage of the Ga droplets. Anisotropic growth ceases under higher NH_3 flows, producing facetted GaN crystallites. In our system it was determined that a TMGa flow of 2.3 μmol/min and NH_3 flow of 20 sccm supports a condition that is close to stoichiometry at nominally 900°C.

Maintaining the VLS growth hinges on the identification and retaining of

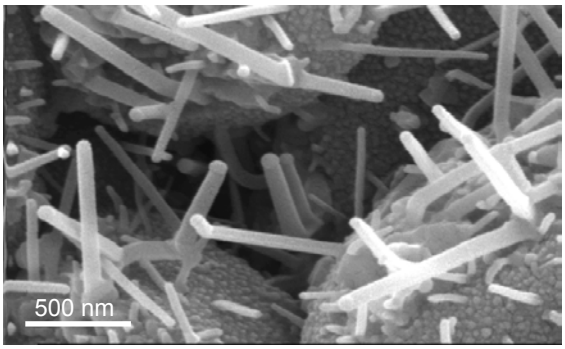

Figure 4. SEM of GaN nanowires using indium catalyst on alumina substrates

stoichiometry due to a strong tendency for GaN to solidify under a nitrogen-rich growth condition.[11] To increase the sustainability of the liquid droplets and alleviate the sensitive dependence on stoichiometry, indium is introduced during the growth of GaN nanowires as a "solvent" agent. InN has a reduced bond energy, and adding indium during GaN growth enhances the thermodynamic tendency of liquid formation over a wide range of ammonia and gallium partial pressures, thus greatly expanding the domain of liquid phase in the alloy phase diagram.[12] A high vapor pressure of indium at typical nanowires growth temperature (10^{-3} ~10^{-2} Torr) implies that most of the indium undergoes steady-state adsorption and desorption processes with very little incorporation. Figure 4 shows GaN:In nanowires on alumina substrates with Ni catalyst after 1 hour of growth with an average diameter of 90 nm and length of 1 to 2 μm. The molar flow ratio between TMIn and TMGa is 10, which is commonly used in the growth of GaInN multiple quantum wells. The use of *in-situ*, desorptive "catalyst" such as indium, in contrast to transitional metal catalysts that are applied prior to growth and float on the nanowires tips, opens up the possibility of a flexible toggling between the VLS and regular VS growth modes. We note in passing that the density of nanowires is relatively low ($<10^9 cm^{-2}$) when compared to that of the catalyst-mediated GaN nuclei, most likely due to the absence of active nucleation sites on the substrates with proper microscopic accommodation, a point to be elaborated in the following.

At the inception of nanowires growth, crystallization at the liquid-solid interface necessitates the formation of a well-defined, low-index interface;[13] the overall crystallographic configuration is based on the statistical minimization of free energy of the combined growth front and side facets based on Wulff theorem.[14] To facilitate the yield and control of nucleation, mesoporous molecular sieves (MCM-41)[15] consisting of hexagonal arrays of silicate materials with well-defined pore sizes of nominally 3.5 nm are employed. Fig. 5 shows an SEM image of In-doped GaN nanowires using identical growth procedure except on MCM-41 templates. The density of nanowires in this case is much increased while the wire diameter is reduced to 30-40 nm. We speculate that the MCM-41 template serves at least two purposes: (1) A surface with high curvature will facilitate the perturbational optimization of crystallographic orientation and enhance nucleation events; (2) A high surface area ($\geq$2000 m^2/g) will prevent the sintering and coalescence of liquid phase droplets and result in a tighter control of the dimensions of

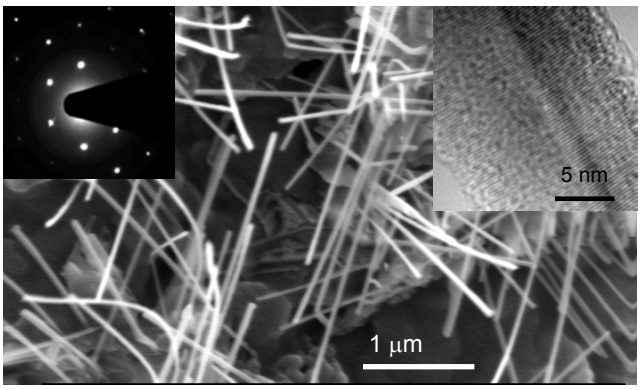

Figure 5. SEM of GaN:In nanowires on MCM-41 templates. Inset: High resolution TEM (right) and electron diffraction images (left)

nanowires. X-ray diffraction 2θ-Ω scans (not shown) confirmed the presence of GaN diffraction peaks. These wires were dispersed through sonication in ethanol onto TEM grids. Selected area electron diffraction (inset of Fig. 5) and SEM indicates the wires are oriented along the [10$\underline{1}$0] direction with a triangular cross-section bound by two {11$\underline{2}$2} and a {0001} planes. The (10$\underline{1}$0) plane (m-plane) has been identified[16] to have the lowest surface energy with the formation of Ga-Ga dimer reconstruction, consistent with the notion that VLS growth proceeds through a Ga-rich liquid-solid interface. The triangle cross section also hints at the compet itive nature of facet growth and the influence of growth conditions on surface energies.[17]

A distinct advantage of using a commercial MOCVD platform is the flexibility of rapid modulation of vapor species for doping and heterostructures. Growth and characterization of $Al_{0.2}Ga_{0.8}N$/GaN nanowire superlattice and doped p-n junction will be reported elsewhere. By replacing TMGa with TMAl of an identical flow rate, we have achieved the synthesis of (Ga-free) AlN nanowires (Fig. 6). The use of indium catalyst remains effective in inducing the 1D growth, evidenced by the droplets at nanowires tips. Having established the synthesis procedures for binary GaN and AlN nanowires, we attempted[18] AlN/GaN superlattice heterostructures toward a proof-of-concept illustration of nanoscopic tailoring by MOCVD. Fig 7a shows an SEM image of these structures,

representing a surprising departure from single 1D nanowires to complicate 3D trunk-branch nanostructures. Selected area electron diffraction indicated that the trunk is consisted of a [10$\underline{1}$0] oriented GaN core (30 nm in diameter), as is described earlier, and an AlN sheath of 5-10 nm thick (Fig. 7b). Roughening in the sheath region was observed under high-resolution TEM, possibly due to highly strained growth of AlN on the GaN facets. Nanoscale compositional analysis by EDS is shown in Fig. 7b and 7c-e, indicating the existence of AlN (or high Al-fraction AlGaN) branches with indium tips. Formation of tree like nanostructures as controlled multiplication of nanowires networks is of contemporary interest[19] and was demonstrated recently through iterative cycles of catalyst applications, VLS synthesis, and growth interruptions. The *in-situ* formation of nano-branches, which does not occur with uniform GaN wires, is likely strain-driven to accommodate elastically the 2.4% lattice mismatch while maintaining the preferential [10$\underline{1}$0] directions for Al(Ga)N nanowires branches. Four of the six equivalent {10$\underline{1}$0} branches are observed that are at approximately 60° or 120° to the trunk, contrasting the

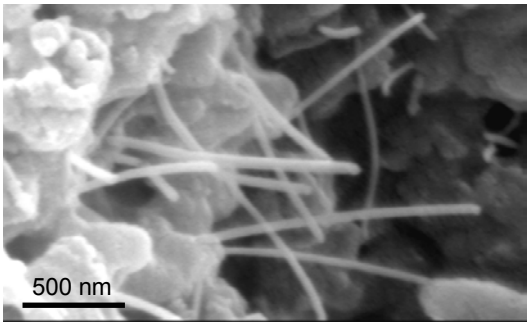

Figure 6. SEM of AlN:In nanowires on MCM-41 templates.

recent reports of 90° nano-branches in cubic Si and InP systems.[19] It also points to a new degree of tunability in constructing complex three-dimensional nanostructures through strain engineering.

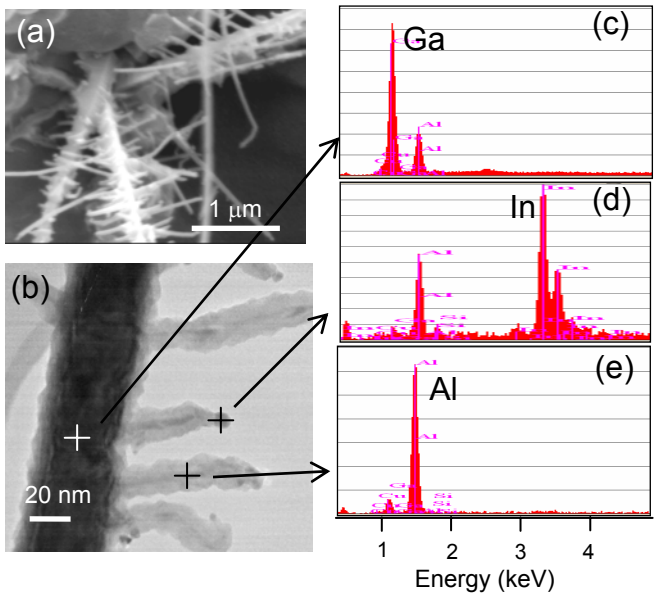

Figure 7. (a) SEM of MOCVD grown GaN/AlN nanostructures using indium catalyst on MCM-41(b) TEM image and selective area EDX showing that (c) the trunk is made of GaN (with an AlN sheath), (d) In droplets still present at the tips of branches, and (e) the branch is mostly AlN.

III. C. Microcavity LEDs

Vertical cavity devices (VCSELs and resonant cavity LEDs) are one class of devices that are attractive for solid state lighting applications at short visible and UV wavelengths due to their directional emission, monochromaticity, and compatibility with multielement array fabrication. In the fabrication of III-nitride-based microcavity devices, several building blocks need to be in place as was illustrated in Fig 8. First, an active region that can efficiently convert the electrically injected carriers into photons needs to be developed. Secondly, the encasing and one-dimensional confinement of photons over the optical wavelengths requires the fabrication of epitaxial distributed Bragg reflectors using AlGaN/GaN. Lastly but by no means the least, the steering of electrical current flow into the center of the cavity, in the presence of using a dielectric top mirror design, mandates the use of an intercavity

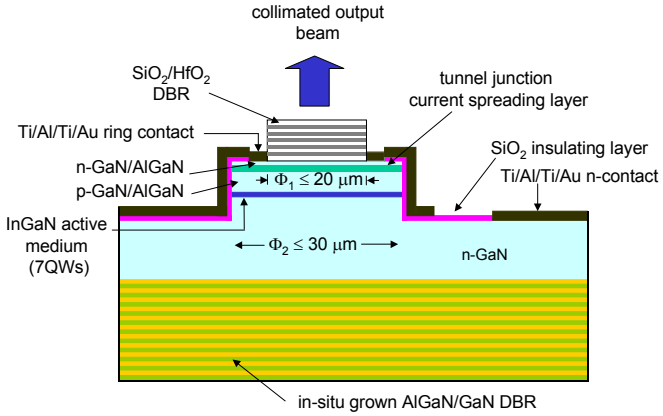

Figure 8: Schematic of an RCLED device with one as-grown GaN/AlGaN and one dielectric DBR mirror,

current spreading scheme such as an Esaki-diode –like tunnel junction. These three directions have been rigorously pursued during the first year and will be described in the following.

1. InGaN-MQW based light emitting medium

After a series of InGaN multiple quantum well calibration growths in December of 2003, we initiated the effort of 410 nm VCSEL in January of 2004 toward the demonstration of electrically injected surface emitting devices. Under optical pumping, a sample with ten

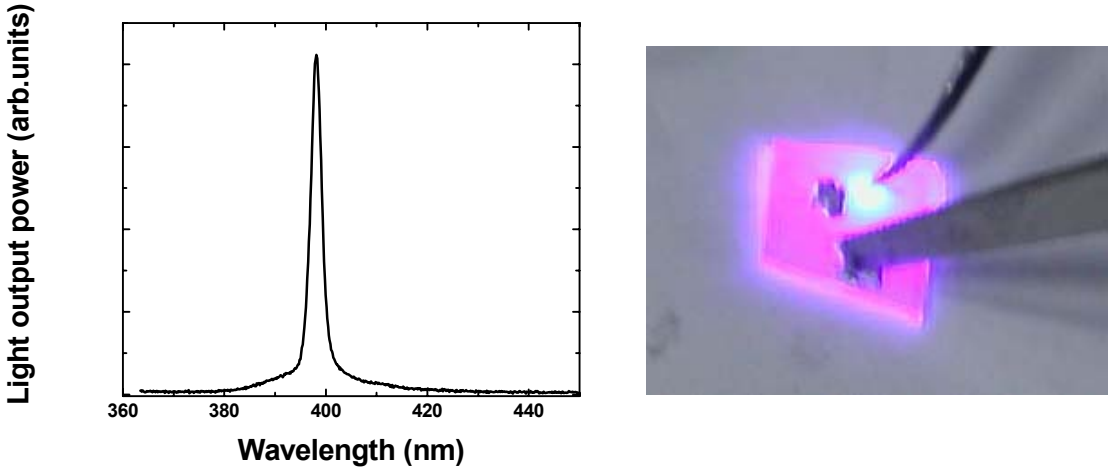

Figure 9. (Left) Amplified spontaneous emission (ASE) from an InGaN/GaN multiple quantum well structure under optical excitation; (Right) Digital images showing LED emission at 410 nm.

InGaN/GaN MQWs exhibited amplified spontaneous emission (ASE, Fig. 9) under relatively low pumping power, indicating the quality of the active region (InGaN MQWs) is sufficient to produce optical gains. Atomistic morphology was study and optimized by varying the growth pressure during the MOCVD process (from 200 to 300 mbar). P-doping of GaN was established and high-brightness LED at 410 nm is achieved (Fig. 9). We are in the process of quantifying the internal efficiency.

2. AlGaN/GaN DBRs

The large number of AlGaN/GaN layer pairs (>50) to achieve the high reflectivities present sizable difficulties in the control of cracks and the DBR morphology. It has been discovered recently[20, 21] that the use of AlGaN interlayers is effective in controlling mismatch-induced stress and suppressing the formation of cracks otherwise occurred during growth of AlGaN directly upon GaN epilayers. During the first year we have completed the growth and calibration of epitaxial AlGaN/GaN distributed Bragg reflectors (DBR) toward the fabrication of 410 nm vertical cavity emitters for enhanced spontaneous emission and light extraction. Important issues related to the DBR growth include 1) Morphological control at macroscopic (mm-scale) and atomistic levels, both are related to the morphology of starting GaN templates, 2) Control of mismatch strain

through the use of interlayers or supperlattices, and 3) N-type doping to enable current injection through the mirror. We achieved in this year the growth of 20-pair AlGaN (35%)/GaN DBRs with good morphology (under Nomarski microscope as well as AFM) and tunable reflectance peak from 390 nm (Figure 10) to 440 nm (not shown) by changing the periodicity of the DBR layers. A 90% peak reflectance and stop bandwidth of almost 20 nm have been achieved. The use of stress-control AlN interlayer helps to eliminate all the crackings. It is our opinion that the epitaxial DBR mirror has reached a level that can support serious VCSEL pursuit.

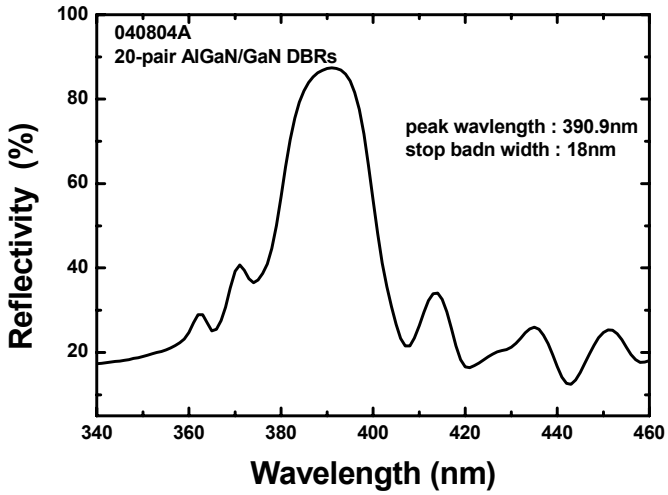

Figure 10. Refectivity spectra of 20-period Al0.35Ga0.65N/GaN DBRs with thickness of period of 74.1 nm

3. Tunnel junction

To counter the high resistivity associated with p-(Al)GaN layers and the need for lateral current spreading into the center of microcavity, a conducting intra-cavity current spreading layer is required. Previously we used indium-tin-oxide, which has only a limited transparency at 400 nm. An Esaki-type tunnel junction is an effective way to contact p-GaN and spread current laterally through a degenerately doped n++GaN layer. Two samples were grown that consist of InGaN based 410 nm LED and capped with p+/n+ tunnel junctions. Initial characterization indicates that the operating voltage at 20 mA (under a quick, mesa-free testing configuration) increases from 5-6 V to 20 V. Resistivity measurement from the surface layers suggest the n+GaN is surprisingly resistive (~150 Ω from two-probe experiment), suggesting that the concentration of silicon dopant is not optimized. SIMS results reveal two problems associated with the tunnel junction formation: 1) The Mg-memory effect causes a slow decay of the Mg-doping (black squares) profile into the n++ region (shaded red region), and 2) an insufficient incorporation of silicon (blue triangles) into the n++ region. These issues will be addressed in the coming months.

III.D. Nanolithography of AlGaInN media

In this work, we fabricated arrays of nanoposts from InGaN/GaN MQW heterostructures, following in part process techniques initiated in earlier work [2]. We concentrated on heterostructures that emitted in the λ=410 nm and 460 nm regimes, due to the importance of these wavelengths for violet lasers and blue LEDs, respectively. The active medium of

a typical λ=410 nm heterostructure was composed of InGaN QWs (x_{In}=0.06) with 33 Å well and 64 Å barriers, grown atop a 200nm thick n-type doped GaN lower cladding layer and a 2 μm thick GaN buffer layer on a sapphire substrate. The top cladding layer was relatively thin, about 20nm of AlGaN (x_{Al}=0.07) to facilitate the etch-based formation of the nanoposts described below. The λ=460nm structures followed a comparable design, with correspondingly larger In composition in the QWs.

The fabrication employed electron beam lithography to first generate patterned PMMA as a template. The e-beam writing of sub-100 nm size patterns atop the insulating sapphire is challenging due to electrostatic charging problems. After writing, the patterns were transferred onto the nitride heterostructure to generate arrays of nano-size posts by reactive ion etching (RIE) in an Ar/Cl_2 mixture with nickel-based etching mask. Typical etch depth was on the order of 300 nm to ensure that the etching reached well below the MQW active regime. The RIE etching condition was optimised so that smooth vertical sidewalls defined the individually isolated MQW nanoposts. Figure 11 shows scanning electron beam microscope images of one high-density square array at two different levels of magnification. Array sizes up to about 60μm x60μm were fabricated.

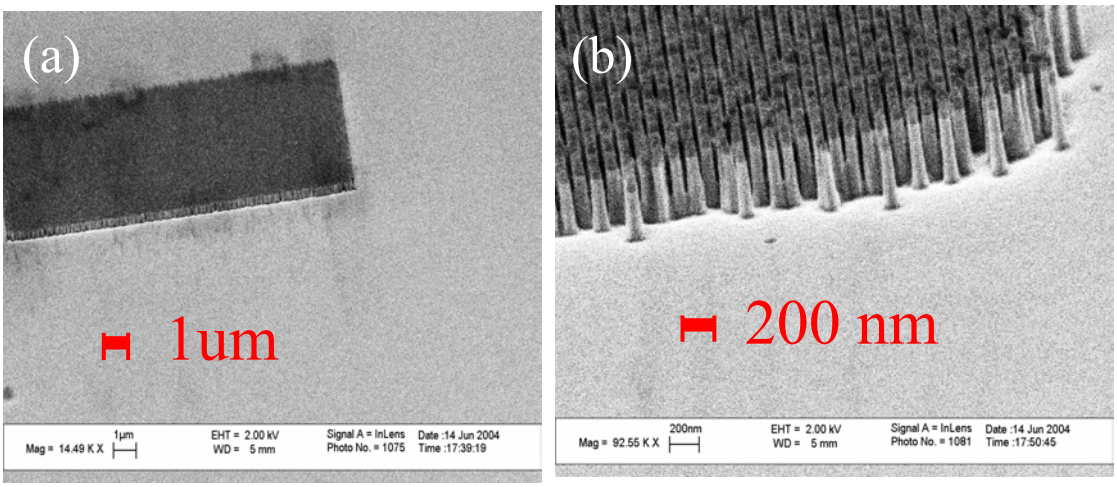

Fig. 11. (a) Global view of patterned InGaN MQW nanoposts (a shadow in the image is due to charging effect in the electron microscope); (b) Image under higher magnification of 60nm diameter nanoposts with approximated 30nm edge-to-edge separation.

We also investigated other array geometries such as hexagonal lattices arrays and quasi one-dimensional arrays (see Figure 12 (a) below), with varying nanopost diameters and their center-to-center separation. In this paper, we will concentrate on three patterned structures: (A) a square-lattice array of 70nm diameter nanoposts with 120nm center-to-center separation etched from the λ=410 nm InGaN MQW wafer; (B) a square lattice array of 40nm diameter nanoposts with 80nm center-to-center separation etched from λ=460nm InGaN MQW wafer; (C) a quasi-one dimensional linear array of 40nm diameter nanoposts with 80nm center-to-center post separation and 320nm separation between the arrays, also embedding the λ=460nm MQWs.

III.E. Mesoscopic media- NanoELO

Silicon dioxide masks (~70nm) were deposited on AlGaN epilayer, upon which nanometer-size windows with varying sizes and densities were patterned through e-beam lithography. Re-growth was performed that consisted of three InGaN MQWs at low temperature followed by HT GaN growth. This growth serves to establish the baseline of the ELO growth condition. (see adjacent SEM image of the first attempts at regrowth).

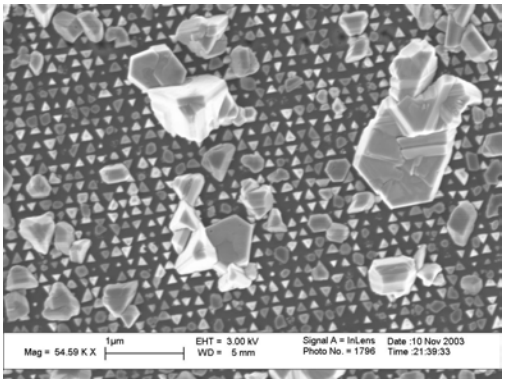

III.F. Superluminescence medium

It is by now fairly well established that nonradiative recombination at free surfaces of GaN and its alloys does not dominate electron-hole pair dynamics to the same degree of severity as with 'conventional' III-V semiconductors. This seminal behavior is a combination of the innate ability of the nitride surfaces to reconstruct so as to remove the surface Fermi level from the bandgap, and the short e-h diffusion lengths due to carrier localization in InGaN QWs (from pronounced alloy potential fluctuations). Here we are able to infer such a conclusion quite directly by employing the very small laterally

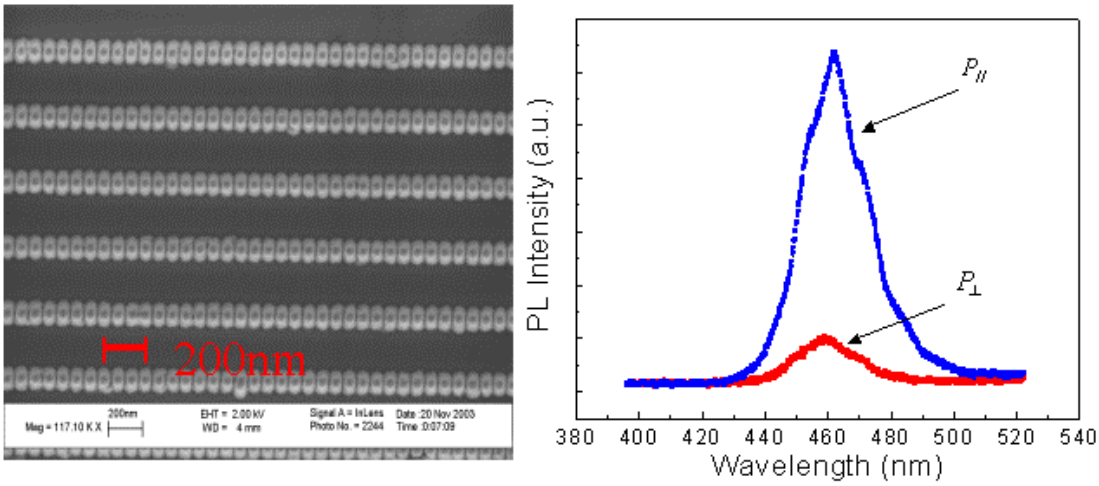

Figure 12. (a) Electron microscope top view of linear InGaN nanopost arrays C. (b) Polarized spontaneous emission from such arrays, demonstrating clear emission **anisotropy.**

patterned structures with their large surface-to-volume ratio, where the free surfaces have been prepared by a dry etching process that involves both chemical and physical factors in exposing the QW (and adjacent GaN sidewalls) to free space. The data of relative luminescence efficiency and lifetime measurements suggests that radiative recombination remains the dominant process for the e-h pairs in the patterned nanopost samples. Further, earlier investigations have shown that excitation levels employed in our measurements correspond to the situation where the localized states in the InGaN QWs

are most likely filled and the e-h pairs reside in extended states, thus well within the diffusion length from the nanopost surfaces.

The potential for near-field effects has also been studied in linear nanopost arrays of InGaN heterostructures as shown in Figure 12. Again, the light emission efficiency remained high in the patterned structure; however, its spontaneous emission characteristics now displayed strong preferred linear polarization along the axis of the array, as shown in Figure 12 (b). It appears that near-field nearest neighbour electromagnetic interaction plays a role in coupling the emission of adjacent nanoposts given their expected large dipolar strength, in rough analogue to Forster energy transfer in molecular dyes. This issue is expected to be of seminal importance in the future biofabricated semiconductor nanocrystalline arrays whether employed as absorbers of photons or/and as material from which electronic excitation can be effectively transferred to other functional elements of the nanocomposite solar cell.

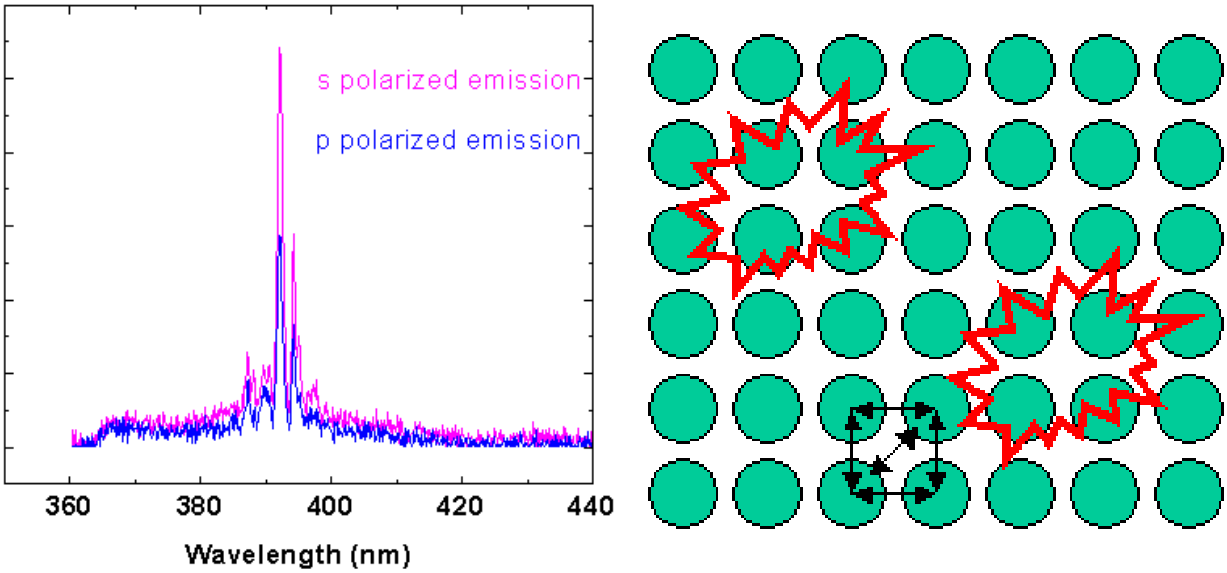

Figure 13. (left) Stimulated emission from InGaN "nanolaser"; (right) cartoon illustrating the photon localization concept to produce short photon mean free paths in high gain media.

Remarkably, the dense square nanopost arrays, such as in Fig. 12 also demonstrate a propensity for stimulated emission (or "lasing") under rather modest (optical) excitation conditions. Figure 13 shows the emission spectrum acquired by optical pumping of the nanopost array over a micrometer scale lateral area. Closer examination under high resolution microscopy has indicated that stimulated emission occurs in "local neighborhoods" that appear to involve small clusters of nanoposts, within which photons are recycled and amplified. At one level, the heterogeneous nanoscale material, with strong light wave scattering, induced by the sub-wavelength structure, can provide for such photon localization which in the presence high gain can be envisioned to lead to an effective local feedback, i.e. structurally enlarging the effective local dipole moment.

Beyond such simple photon localization, which correspondingly the effective absorption coefficient for nanostructured material in a solar cell application by photon recycling, the physics of light-matter-interaction of this type of nanoscale materials will be sought to have another fundamental advantage via near-field dipole-dipole interaction (photon tunneling) between adjacent nanocrystal elements. If coherent, the process can produce a giant (dipolar) oscillator strength associated for both light absorption and emission, concentrated within a designed spectral bandwidth. Such collective excitonic enhancements will be of importance in endowing nanoparticle arrays optoelectronic assets not available in normal semiconductor materials.

III.G. Photonic Crystal

We have fabricated and characterized a light emitting photonic crystal slab in the blue near 460 nm, based on InGaN quantum well active material. A multilayer nanopattern transfer technique was developed to fabricate these optical structures. The dependence of the photoluminescence enhancement on specific pattern dimension, coupled with distinct polarization characteristics of emission, was found to be in good agreement with theoretical simulations, thereby supporting the existence of photonic crystal bandgap. The results suggest that practical fabrication of a photonic crystal slab-type light emitting diodes for enhanced external quantum efficiency in the blue and ultraviolet is feasible.

Samples for this study were grown by MOCVD and were composed of three pairs of InGaN/GaN QWs (40Å QW/60Å barrier) for near 460 nm emission, embedded approximately 80nm below the surface by a GaN capping layer. To guide the PC slab design, we performed a three-dimensional finite-difference time-domain (3D FDTD) analysis of in-plane propagation of a simulated test light pulse for our heterostructure. The pulse was launched at the center of the PC slab and its transmission spectrum after propagating a distance of five PC lattice constants was calculated in the frequency domain. A specific case, namely a hexagonal lattice structure was composed of 120nm airholes of diameter and a 159nm lattice constant to achieve largest bandgap for the TE mode (from about 350nm to 500nm), including the targeted emission wavelength. The etch depth of the airholes was chosen to be three times the lattice constant to ensure a good light extraction efficiency, while increasing the actual PC slab fabrication challenges. Hence the airholes penetrated the InGaN/GaN QWs so that the active medium lies physically within the 2D PC slab.

In terms of actual fabrication, high etch selectivity and good etch anisotropy are prerequisites for transferring the designed nanopatterns into the III-nitride material with requisite fidelity. The starting pattern was generated on a thin (~80nm) PMMA film by electron beam lithography. Due to the fragility of PMMA, a specialized multilayer pattern transfer technique was developed to subsequently imprint the nanopattern onto the nitride heterostructure. Each layer of the intermediate etching masks, including germanium, polymer, titanium and SiO_2, played a role in creating a hard mask for the final etching process, while preserving the nanopattern with minimum degradation. Specifically, the use of a thin layer of germanium underneath the thin top PMMA layer not only reduces the charging effect in electron beam lithography but also serves as a

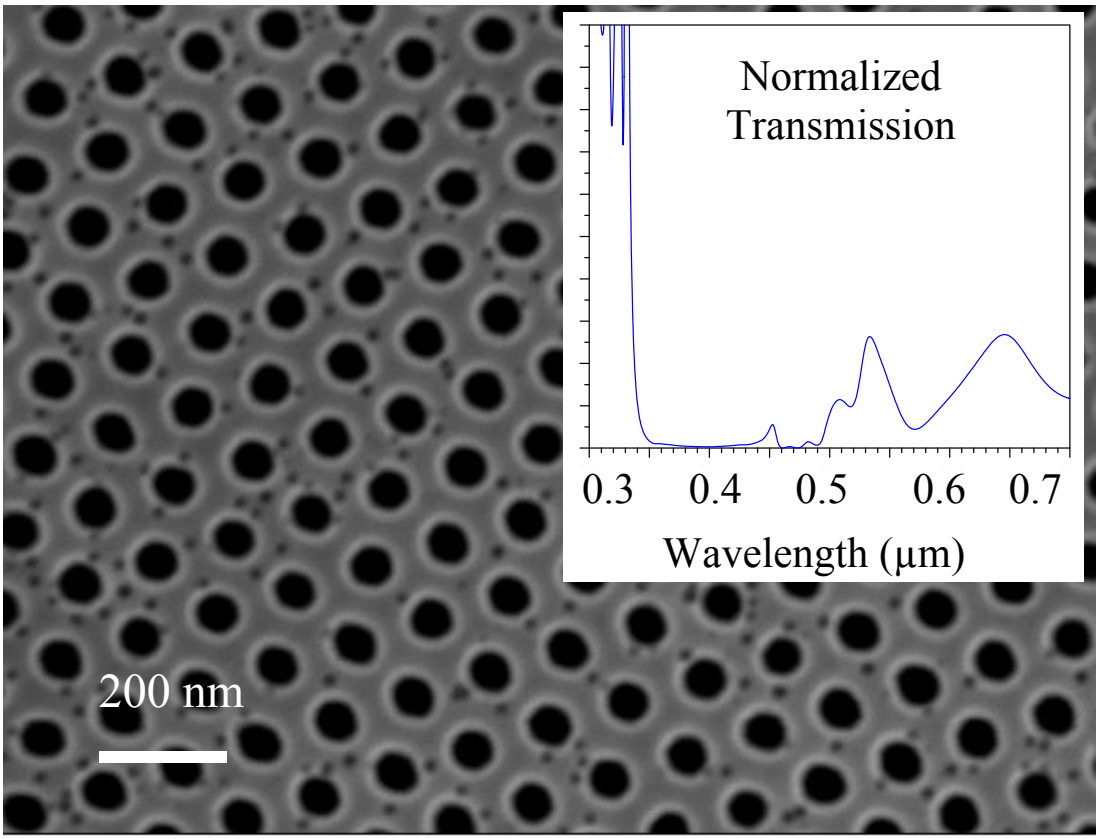

Figure 14: SEM image of InGaN/GaN QW photonic crystal slab fabricated by the multilayer nanopattern transfer technique (hexagonal lattice of 120nm air hole diameter and 159nm lattice constant). The inset shows a 3D FDTD simulation of the transmission spectrum for in-plane lightwave propagation.

mask for subsequently transfer of the PC airhole pattern onto a thicker and more robust polymer layer. The pattern created within the polymer layer was in turn transferred onto a titanium thin film by reactive ion etching (RIE) in Cl_2 and then onto a SiO_2 film by a CHF_3 RIE step. The particular choices of the RIE processes and use of intermediate mask material enabled the creation of a thick hard SiO_2 mask for final nitride etching by an Cl_2 electron cyclotron resonance tool (ECR). An SEM image of a final nitride photonic crystal slab is shown in the top of **Figure 14**. We have generalized this nanofabrication technique and applied to both various GaN-based and silicon wafers to create patterns with feature size as small as 40nm.

The light emission properties of the InGaN/GaN MQW PC slabs were studied by simple photoluminescence (PL) techniques, by employing a short (psec) pulsed laser source at $\lambda = 400$ nm, with the beam focused normally incident on the sample surface to a 5um spot. The excitation level was adjusted to approximately $1\mu J/cm^2$ per pulse in the experiments described next; the excitation level dependence of the PL from the PC slab will be commented briefly later in this letter. The PL was collected by an objective with a numerical aperture of 0.85 N.A. and detected through a spectrometer in the transmission-

type geometry. In this geometry, where the pump laser is incident on photonic crystal slab from the GaN cap layer side and the PL is collected through the sapphire substrate, the InGaN/GaN QW photonic crystals of optimal design exhibit considerably enhanced photoluminescence, eight-fold relative to the PL measured from unpatterned area under the same pumping condition, as shown in **Figure 15**. This is believed to be the highest far-field light emission enhancement reported on blue III-nitrides so far. A strong dependence of the extraction efficiency on the air hole diameter was measured (for a fixed lattice constant), with the best enhancement achieved for structures with the diameter of the air hole between 100nm and 120nm, in good agreement with the simulation predictions. By comparison, when the sample was flipped so that pump light was now incident from the substrate side (i.e. the PL was collected from GaN cap layer side), the enhancement relative to the unpatterned wafer was reduced to a factor of three. This interesting contrast can be explained noting the dielectric asymmetry of our photonic crystal. The large index of refraction difference between air and GaN (n~2.5) provides a strong confinement at the sample surface, while on the substrate side the interface is between a thick (~ 2 μm) GaN bottom buffer layer and the PC slab. Calculations by Ryu et al by the 3D FDTD method have shown that the efficiency of light extraction into air from a PC slab decreases distinctly as the index of the bottom cladding layer increases, while the total extraction efficiency (contributions to emission from both surfaces) remains constant.

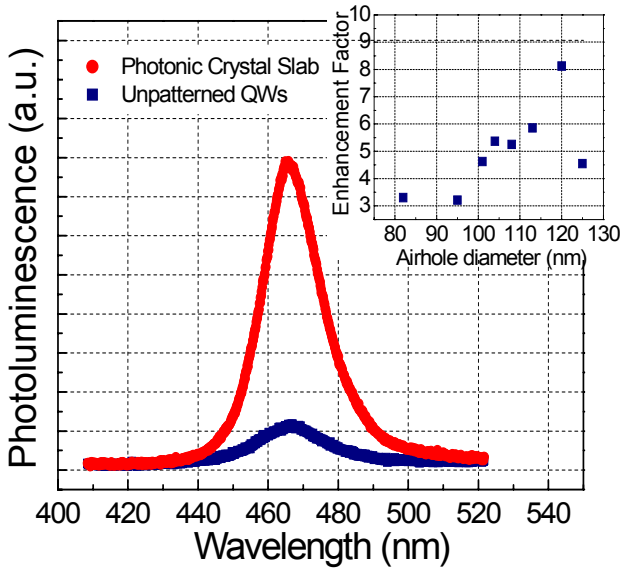

Figure 25: Enhancement of emission spectra from photonic crystal relative to unpatterned QW sample. Inset shows the dependence of the enhancement on the air hole diameter.

IV. PROBLEMS ENCOUNTERED

GaN/Air DBR: Due to a very large contrast in the indices of refraction between air (n=1) and GaN (n~2.4), it was proposed that fabrication of a novel air/GaN DBR represents an efficient approach to build up the optical interference within a short distance, thus enabling the possibility of λ-cavity that is important for microcavity. The implementation of this idea is based on the selectivity of photo-enhanced chemical etching (PEC) of GaN and AlGaN. In this case minority carriers (holes) created by the above-bandgap excitation assists the oxidation and etching process. While we demonstrated the PEC etching of GaN and AlGaN, it was discovered that the selectivity

is insufficient; etched surfaces of GaN (and AlGaN) do not possess optical smoothness that is needed for DBR mirrors. Currently, we are pursuing the concept of external cavity with two dielectric mirrors (top and below substrates) and one epitaxial mirror that relieves the stringent demand on the reflectivity and material quality. In this case a reflectivity of 60 to 70% is adequate.

VI. SIGNIFICANT ACCOMPLISHMENTS

In the past 12 months we have :

- Developed new means of gallium nitride quantum dot synthesis by the technique of droplet heteroepitaxy
- Developed a vapor-liquid-solid based approach to synthesis of AlGaN and GaN nanowires
- Fabricated high-reflectivity distributed Bragg planar components for vertical microcavity emitter applications in the violet.
- Designed and fabricated photonic crystal structures near 460 nm blue wavelength and achieve a 8-fold increase in spontaneous emission efficiency
- Developed a fabrication approach to light emitting InGaN quantum well nanoarrays in the 410 nm region
- Demonstrated stimulated emission from the 410 nm nanoarrays

VII. LIST OF PUBLICATIONS AND PRESENTATIONS

Presentations:

- J. Han, "III-N Exploratory Devices and Nanostructures", seminar at Princeton University, May 2004.
- J. Han, "III-N Exploratory Devices and Nanostructures", seminar at Paul Drude Institute, Berlin, Germany, May 2004.
- J. Han, "III-N Exploratory Devices and Nanostructures", seminar at EPFL, Lausanne, Switzerland, May, 2004.
- M. Gherasimova et al, "Fabrication of GaN Quantum Dots on AlGaN Template by Liquid Droplet Epitaxy", presented at EMC, Notre Dame, Indiana, June, 2004
- J. Su et al, "MOCVD Growth and Characterization of GaN nanowires", presented at EMC, Notre Dame, Indiana, June, 2004.
- M. Gherasimova et al, A nanocluster route to zero- and one-dimensional quantum structures by MOCVD", presented at International Workshop of Nitride Semiconductors, Pittsburgh, PA, July 2004.
- J. Han, "MOCVD Growth of III-Nitride Nanostructures", 2004 UKC Conference, Research Triangle, NC, August 2004.

- J. Han, "MOCVD Growth of III-Nitride Nanostructures", AFOSR Workshop, Anchorage, AK, August 2004.
- A. Nurmikko and J. Han, "Ultraviolet LEDs for Versatile Applications", ISBLLED, Gyongju, Korea, March 2004
- L. Chen et al, "Photonic Crystals in InGaN Light Emitters", CLEO, San Francisco, June 2004
- Y. He, et al, "Optical Properties of Sub-100nm Diameter Nanoposts with Embedded InGaN Quantum Well Heterostructures", presented at International Workshop of Nitride Semiconductors, Pittsburgh, PA, July 2004
- L. Chen et al, "High Efficiency Photonic Crystals in InGaN Light Emitters", presented at International Workshop of Nitride Semiconductors, Pittsburgh, PA, July 2004

Publications:

- M. Gherasimova et al, "Droplet Heteroepitaxy of GaN quantum dots by MOCVD", accepted for publication in APL.
- J. Su et al, "Catalytic Growth of AlGaInN Nanowires and Nanostructures by Metal-Organic Chemical Vapor Deposition", submitted to APL.
- J. Su et al, "Selectively Epitaxial Growth of Aligned AlGaInN Nanowires by Metal-Organic Chemical Vapor Deposition", submitted to APL.
- J. Han and A. V. Nurmikko, "Wide Band Gap III-Nitride Semiconductors", McGraw-Hill 2004 Year Book of Science and Technology
- M. Gherasimova et al, "A nanocluster route to zero- and one-dimensional quantum structures by MOCVD", submitted to phys. Stat. Sol.
- Yiping He et al, "Optical Properties of Sub-100nm Diameter Nanoposts with Embedded InGaN Quantum Well Heterostructures", submitted to Phys. Stat. Sol(a) (2004)
- "Fabrication and Performance of Efficient Blue Light Emitting III-Nitride Photonic Crystals", Lu Chen and A.V. Nurmikko, Appl. Phys. Lett. (in press 2004)

VIII. APPROACHES TO BE TAKEN IN THE FOLLOWING YEAR

In the next 12 month contract period we will:

- Evaluate and incorporate GaN-based quantum dots as active media in light emitter heterostructure device structures

- Insert our newly developed quantum wires onto organized templates for high density nanoscale arrays, and investigate the light emission enhancement in such novel architectures

- Develop both the distributed Bragg reflector and tunnel junction components and assemble these for a vertical resonant microcavity LED

- Imbed the lithographically fabricated nanopost arrays into LED-type devices and develop a process technology for electrical injection

- Investigate the feasibility of using the recently observed stimulated emission from InGaN QW nanopost arrays as an enabler for a new generation of laser devices at short visible wavelengths.

IX. CONCLUSION

We have reported on research results in this project which synergize advanced material science approaches with fundamental optical physics concepts pertaining to light-matter interaction, with the goal of solving seminal problems for the development of very high performance light emitting diodes (LEDs) in the blue and near ultraviolet for Solid State Lighting applications. Accomplishments in the first 12 month contract period include (i) new means of synthesizing zero- and one-dimensional GaN nanostructures, (ii) establishment of the building blocks for making GaN-based microcavity devices, and (iii) demonstration of top-down approach to nano-scale photonic devices for enhanced spontaneous emission and light extraction. These include a demonstration of eight-fold enhancement of the external emission efficiency in new InGaN QW photonic crystal structures. The body of results is presented in this report shows how a solid foundation has been laid, with several noticeable accomplishments, for innovative research, consistent with the stated milestones.

X. REFERENCES

[1]S. Iijima, Nature 354, 56 (1991).

[2]Y. Cui, L.J. Lauhon, M.S. Gudiksen, J. Wang, C. M. Lieber, Appl. Phys. Lett. **78**, 2214 (2001).

[3]B. J. Ohlsson, M. T. Björk, M. H. Magnusson, K. Deppert, and L. Samuelson, Appl. Phys. Lett. **79**, 3335 (2001); M. Yazawa, M. Loguchi, A. Muto, M. Ozawa, and K. Hiruma, Appl. Phys. Lett. **61**, 2051 (2001); X. Duan, and C.M. Lieber, Adv. Mater. 12, 298 (2000); X. Duan and C. M. Lieber, J. Am. Chem. Soc. 122, 188 (2000).

[4]R. S. Wagner in *Whisker Technology*, edited by A. P. Levitt, John Wiley & Sons, New York (1970)

[5]P. A. Smith, C. D. Nordquist, T. N. Jackson, T. S. Mayer, *Appl. Phys. Lett. 77*, 1399 (2000); Y. Huang, X. Duan, Q. Wei, C. M. Lieber, Science 291, 630 (2001); D. Whang, S. Jin, Y. Wu and C.M. Lieber, Nano Lett. **3**, 1255 (2003).

[6]Y. Wu, R. Fan and P. Yang, Nano Lett, 2, 83 (2002).

[7]M. T. Björk, B. J. Ohlsson, T. Sass, A. I. Persson, C. Thelander, M. H. Magnusson, K. Deppert, L. R. Wallenberg and L. Samuelson, Appl. Phys. Lett. **80**,1058 (2002).

[8]For example, C. Chen, C. Yeh, C.Chen, M. Yu, H. Liu, J. Wu, K. Chen, L. Chen, J. Peng,and Y Chen, J. Am. Chem. Soc., 123, 2791 (2001).

[9]G.B. Stringfellow, Mat. Sci. and Eng. B 87, 97 (2001).

[10]Sapphire, alumina, SiO_2, and MOCVD-grown GaN epilayers were dipped in 0.01M $Ni(NO_3)_2$ aqueous solution and dried in air on filter papers before loading into the MOCVD reactor.

[11] While the catalytic effects of transitional metals are well established, there is little evidence that these metals (Au, Ni, and Fe, for example) form a eutectic system with GaN with self-regulatory stabilization of liquid alloy droplets.

[12]A. Koukitu, N. Takahashi, T. Taki, and H. Seki, J. Cryst. Growth, 170, 306 (1997).

[13]K.A. Jackson in *Growth and Perfection of Crystals*, edited by Doremus, Roberts, and Turnbull, John Wiley and Sons, New York (1958).

[14]D. Peng, S. Osher, B. Merriman, and J.-K Zhao, Contemp. Math. 238, 251 (1999). The assumption of a near-equilibrium crystal shape can be justified by the overall nanometer scale in consideration and the rapid kinetics under VLS growth.

[15]J. Y. Yang, C. P. Mehnert, and M. S. Wong, Angew. Chem. Int. Ed. 38, 56 (1999)

[16]J. E. Northrup and J. Neugebauer, Phys. Rev. B. 53, R10477 (1996).

[17] K. Hiramatsu, K. Nishiyama, A. Motogaito, H. Miyake, Y. Iyechika, and T. Maeda, phys. stat. sol. (a) 176, 535 (1999)

[18] After growth of GaN nanowires for 30 min, TMGa/TMAl was closed/opened for 1, 2, 4, 8, and 5 minutes, interleaved by 4 min growth of GaN with TMI flowing continuously.

[19]K. A. Dick, K. Deppert, M. W. Larsson, T. Martensson, W. Seifert, L. R. Wallenberg and L. Samuelson, Nature Mat. **3**,380 (2004); D. Wang, F. Qian, C. Yang, Z. Zhong and C. M. Lieber, Nano Letters, 4, 871 (2004).

[20] H. Amano, M. Iwaya, N. Hayashi, T. Kashima, S. Nitta, C. Wetzel, and I. Akasaki, "Control of dislocations and stress in AlGaN on sapphire using a low temperature interlayer", *phys. stat. sol. (b),* vol. 216, pp. 683-689, Nov. 1999.

[21] J. Han, K. E. Waldrip, S. R. Lee, J. J. Figiel, S. J. Hearne, G. A. Petersen, and S. M. Myers, "Control and elimination of cracking of AlGaN using low-temperature AlGaN interlayers," *Appl. Phys. Lett.,* vol. 78, pp. 67–69, Jan. 2001.